Imaging and tracking single fluorescent nanobeads in solution

Qin Yu (余 琴), Chen Wang (王 琛), Li Liu (刘 力), and Guiying Wang (王桂英)

State Key Laboratory of High Field Laser Physics, Shanghai Institute of Optics and Fine Mechanics, Chinese Academy of Sciences, Shanghai 201800

In single-particle tracking (SPT), fluorescence video microscopy is used to record the motion images of single particle or single molecule. Here, by using a total-internal-reflection microscope equipped with an argon ion laser and a charge-coupled device (CCD) camera with high-speed and high-sensitivity, video images of single nanobeads in solutions were obtained. From the trajectories, the diffusion coefficient of individual nanobead was determined by the mean square displacements as a function of time. The sizes of nanobeads were calculated by Stokes-Einstein equation, and the results were compared with the actual values.

OCIS codes: 170.2520, 290.1990.

Single particle tracking (SPT) is the most direct way of studying molecular diffusion. It is based on the analysis of a sequence of fluorescence microscopy images to follow the sub-micron motion of individual probe which generates diffraction-limited spot[1]. A detailed description and further references can be found in the review by Saxton and Jacobson[2]. So far, SPT has found numerous applications in biophysics, including the diffusion movement of fluorescence-labelled lipids or proteins in cell membranes and nucleus[3−5], and the infection pathway of single viruses into a living cell[6].

Einstein's and Stokes' work on the diffusion of particles led to well-known Stokes-Einstein equation giving the diffusion coefficient D of a sphere:

$$D = \frac{kT}{\xi}, \tag{1}$$

where k is the Boltzmann constant, T is the absolute temperature, and ξ is the fraction coefficient. For translational diffusions, the diffusion coefficient is

$$D_{\rm t} = \frac{kT}{6\pi\eta r}, \tag{2}$$

where r is the radius of the sphere. By means of a fluorescent probe, fluorescence techniques permit evaluation of the fluidity of a microenvironment, and thus diffusion coefficients reveal the structure of plasma membrane, or mesoporous materials.

Total internal reflection fluorescence microscopy (TIRFM), also termed evanescent wave microscopy[7], can enable the direct observation of the motion of macromolecules in plasma membrane. There has been a recent surge in the popularity of this technique in many applications. An important property of the evanescent wave is that the intensity falls off exponentially away from the coverslip. The theoretical penetration depth is 100 nm. Then only a thin layer of fluorophores near the coverslip are excited. For this reason, the signal-to-noise ratio (SNR) is much better and the cellular photodamage and photobleaching are minimal.

Fluorescent nanobeads are fine labels because they neither photobleach nor optically saturate at reasonable exciting intensities. In this paper, 40-nm yellow-green fluorescent beads (505/515, Molecule Probe, Eugene, OR) were injected in 80% glycerol-water mixture (solvent viscosity $\eta = 47$ cPoise[8]), with a final concentration of 1.83 nmol/L, then were dispersed well by sonication for 30 min and by vigorous shaking. Samples were mounted on an Olympus IX-71 objective-type total internal reflection (TIR) microscope and were excited by a linearly polarized 488-nm argon laser (Melles Griot, 35LAP). Fluorescence was collected by Olympus Planapochromat 60×/1.45 oil objective. Images were captured by a charge-coupled device (CCD) camera (Roper Scientific, Trenton, NJ) with 1392×1040, 6.45 μm square pixels, allowing continuous imaging with no interframe dead time.

Images were acquired by Metavue 4.6.5 software (Universal Imaging Co., PA), then were processed and analyzed by a Matlab fit (the program was written with Matlab by the authors). The theoretical distribution of the diffraction-limited spot is to be an Airy disk, but a Gaussian profile is chosen for simplicity, because the differences between two models are minor in practice[9]:

$$I(x,y) = A_n \exp\{-[(x-x_n)^2 + (y-y_n)^2]/2\sigma_n^2\}, \tag{3}$$

A_n is the amplitude of the Gaussian, σ_n is related to the full-width at half-maximum (FWHM) by $\mathrm{FWHM} = 2(2\ln 2)^{1/2}\sigma_n$, x_n, and y_n give the locations of the fitted spots. The errors in the four parameters A_n, σ_n, x_n, and y_n vary for each analyzed spot because the fitting accuracy depends on the SNR. The result of this fitting involves a sequence of positions for each tracked nanobead, which result in the trajectories of the individual nanobead.

The diffusion of single nanobead can be considered as a two-dimensional (2D) random walk[10], in which the mean-square displacement (MSD), $< r^2(t) >$ obeys

$$< r^2(t) >= 4Dt, \tag{4}$$

Generally, MSD(t) can be computed from the formula.

$$\mathrm{MSD}(m\delta t) = \frac{1}{N-m}\sum_{j=1}^{N-m}\{[x(j\delta t + m\delta t) - x(j\delta t)]^2 + [y(j\delta t + m\delta t) - y(j\delta t)]^2\}. \tag{5}$$

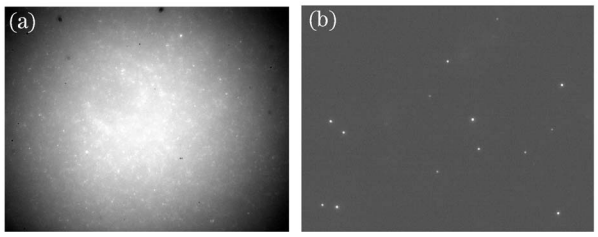

Fig. 1. Images of fluorescent nanobeads with epi-fluorescence and TIR fluorescence. Note that the epi and TIR images are very different (even though the focal plane was not changed).

The MSDs for every time $t = m\delta t$ (m is the number of frames between two positions and δt the acquisition time; N is the total number of images in the recording sequence, and m, j are positive integers with m=1, 2, ..., ($N-1$)) are obtained directly from the trajectory, assuming that any starting point in the trajectory is equally valid. A linear regression between the MSD and t for this trajectory can give the diffusion coefficient D. Then the radius of the nanobead r is derived from Stokes-Einstein equation.

Our aim is to use evanescent-field illumination to selectively excite a thin layer of nanobeads near the coverslip. At the same time, epi-illumination was also done for contrast. Figure 1 shows images of epi-fluorescence and TIR fluorescence individually. It is visible that TIR fluorescence-image appears higher SNR. With TIR fluorescence, the spheres off focus appear dimmer, reflecting the weaker evanescent field at that distance. To analyze the diffusional motion of the nanobeads, 15 beads were selected for data analysis. First, each stack of images was processed by a mean filter. For tracking, we selected the brighter beads that did not collide with neighboring bead during the recording period. In the resulting images, the center locations of the beads were determined by a 2D Gaussian curve fit to the diffraction-limited spots using nonlinear least-squares. The CCD pixel size (6.45 μm) corresponded to 108 nm ($=\frac{6.45}{60}$ μm) in object space. The standard deviation of the 2D Gaussian profile was determined by the above fitting result, and resulted in $<\sigma_n>=136$ nm, corresponding to a FWHM of 320 nm ($\sim$3 pixels). Figure 2 shows surface plots of background subtracted and Gaussian-fitted fluorescent spot from single fluorescent nanobead.

Generally, SNR can be defined as[8]

$$\mathrm{SNR} = \frac{I_0}{\sqrt{\sigma_{\mathrm{bg}}^2 + \sigma_{I_0}^2}}, \tag{6}$$

where I_0 is the maximum signal intensity above background, σ_{bg}^2 is the variance of the background intensity, and $\sigma_{I_0}^2$ is the variance of the maximum signal intensity above the background. From the above fitting result of $<\sigma_{I_0}^2>=6.5$ and $<\sigma_{\mathrm{bg}}^2>=1.5$, and for a mean maximum intensity of 42, the SNR of single nanobead is approximately 6.

The standard deviations of the locations which represent the localization accuracy were calculated. Thompson *et al.* defined a 2D localization accuracy of the spots as[11]

$$<\sigma>^2 = \frac{s^2 + a^2/12}{N} + \frac{8\pi s^4 b^2}{a^2 N^2}, \tag{7}$$

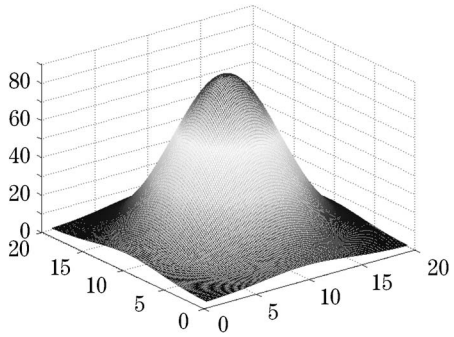

Fig. 2. Surface plots of background subtracted and Gaussian-fitted fluorescent spot from single fluorescent nanobead.

where $<\sigma>$ is the mean error in localization, s is the size of the spot, a is the size of the pixel, b is the background noise, and N is the number of photons collected. For an integration time of 20 ms, the pixel size of 64.5 nm, $<s>=<\sigma_n>=136$ nm, $<N>=33000$ photons, $<b>=108$, therefore, on the average, single nanobead can be localized with an accuracy of 5 nm under the chosen imaging conditions.

We obtained a series of space-time coordinates, which represents a 2D projection of their three-dimensional (3D) trajectory. Figure 3 shows 6 frames of images in a stack of 100. Although a little step movement is apparent in the images, the movie showed that the nanobead was in random walk. Figure 4 shows a trajectory contains 100 positions and displays visible mobility.

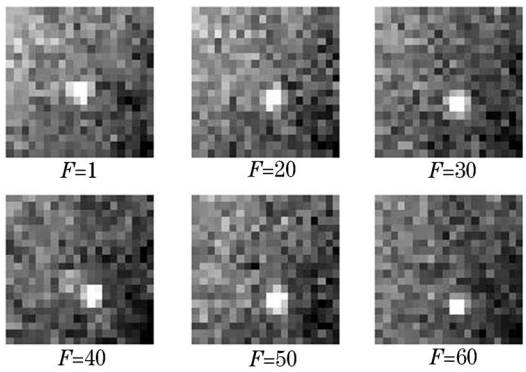

Fig. 3. Six frames of total 100 frames from fluorescence images of single nanobead, showing diffusion in 80% glycerol-water mixture.

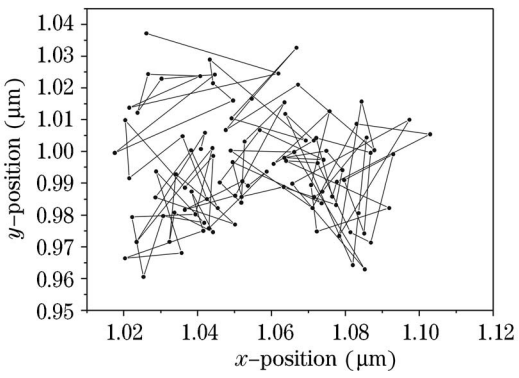

Fig. 4. SA 100-step trajectory of a single nanobead. The integration time was 100 ms.

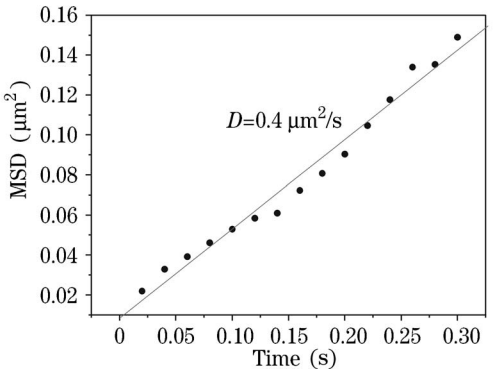

Fig. 5. Mean square displacements (MSDs) of single nanobead as a function of time. The integration time was 20 ms. Temperature was 25 ± 1 °C.

Then, if the spheres move by free diffusion in solution, their average 2D MSD is related to the diffusion coefficient D. We calculated the trajectories of 15 single nanobeads, respectively, and plotted the MSD against time (Fig. 5) By fitting a straight line to the data, we determined an average diffusion coefficient of $D = 0.4$ μm^2/s for $\eta = 47$ cPoise.

Finally, we calculate the radius of the nanobeads in the solution according to the Stokes-Einstein equation, $r = {}^{kT}/_{6\pi\eta D}$. The result is $r = 11 \pm 1$ nm. Error estimations are due to uncertainties in temperature of $\pm 1°$ (an error in glycerol concentration was not considered). The values may appear smaller than the actual value, but they indeed at the same order of the magnitude.

In conclusion, in combination TIR microscopy with SPT techniques, the diffusion coefficients of the nanobeads were derived from MSD(t), and then the sizes of the beads were obtained. The localization accuracy of 5 nm confirms that it is possible to detect, image, and track single fluorescent nanobead in real time in solution as long as they stay in the focal plane. The results obtained in this study allow further applications in single-molecule detection in living cellular systems.

This work was supported by the National Natural Science Foundation of China (No. 60078025) and the State Key Development Program for Basic Research of China (No. 2002CB713808). Q. Yu's e-mail address is qinyu@mail.siom.ac.cn.

References

1. M. K. Cheezum, W. F. Walker, and W. H. Guiford, Biophys. J. **81,** 2378 (2001).
2. M. J. Saxton and K. Jacobson, Annu. Rev. Biophys. Biomol. Struct. **26,** 373 (1997).
3. A. Sonnleitner, G. J. Schütz, and Th. Schmidt, Biophys. J. **77,** 2638 (1999).
4. Y. Sako, S. Minoguchi, and T. Yanagida, Nature Cell Biology **2,** 168 (2000).
5. T. Kues, R. Peters, and U. Kubitscheck, Biophys. J. **80,** 2954 (2001).
6. G. Seisenberger, M. U. Ried, T. Endress, H. Buning, M. Hallek, and C. Brauchle, Science **294,** 1929 (2001.)
7. D. Toomre and D. J. Manstein, Trends in Cell Biology **11,** 298 (2001).
8. U. Kubitscheck, O. Kückmann, T. Kues, and R. Peters, Biophys. J. **78,** 2170 (2000).
9. C. Hellriegel, J. Kirstein, and C. Bräuchle, New J. Physics **7,** 23 (2005).
10. J. A. Steyer and W. Almers, Biophys. J. **76,** 2262 (1999).
11. R. E. Thompson, D. R. Larson, and W. W. Webb, Biophys. J. **82,** 2775 (2002).